

# Study of doping uniformity of a 200 kV ion implanter by RBS and sheet resistance measurements

Hui Li<sup>1</sup> · Ze-Song Wang<sup>1</sup> · Sheng-Jun Zhang<sup>1</sup> · Vasily O. Pelenovich<sup>1,2</sup> · Feng Ren<sup>1</sup> · De-Jun Fu<sup>1</sup> · Chuan-Sheng Liu<sup>1</sup> · Zhi-Wei Ai<sup>1</sup>

Received: 18 August 2015/Revised: 20 January 2016/Accepted: 21 January 2016/Published online: 9 May 2016  
© Shanghai Institute of Applied Physics, Chinese Academy of Sciences, Chinese Nuclear Society, Science Press China and Springer Science+Business Media Singapore 2016

**Abstracts** The ion implantation uniformity is of vital importance for an ion implanter. In this paper, we report the, uniformity measurement for a large current ion implanter (LC-16 type) by implanting of 190-keV Ar ions into Si to  $3 \times 10^{16}$  atoms/cm<sup>2</sup>, followed by Rutherford backscattering spectroscopy (RBS) and sheet resistance measurement providing quantitative information on spatial distribution of dopants. The implant doses obtained from RBS at selected points of the sample give a spatial uniformity of <5 %, which are confirmed by the sheet resistance measurement. While sheet resistance is an indirect method for dose evaluation of ion-implanted samples, RBS provides a competent technique for calibration of the ion implantation system. And both measurements show that good uniformity can be achieved for the ion implanter by tuning of the scanning process.

**Keywords** Ion implanter · Rutherford backscattering · Sheet resistance measurements

---

This work was supported by the National Natural Science Foundation of China (Nos. 11405117 and 11205116) and International Cooperation Program of the Ministry of Science and Technology of China (No. 2015DFR00720).

---

✉ De-Jun Fu  
djfu@whu.edu.cn

✉ Zhi-Wei Ai  
azw@whu.edu.cn

<sup>1</sup> Key Laboratory of Artificial Micro- and Nano-Materials of Ministry of Education and School of Physics and Technology, Wuhan University, Wuhan 430072, China

<sup>2</sup> Institute of Ion-Plasma and Laser Technologies, Academy of Sciences of Uzbekistan, Tashkent 700135, Uzbekistan

## 1 Introduction

Ion implantation, which provides a uniform and reliable process for introducing intrusive impurities into target solids and shows much effectiveness in achieving mechanical, electrical and optical properties of materials, is not only used as a standard process in semiconductor industry, but also used in modification of metals and ceramics [1–4]. In particular, to study defects and failure of nuclear materials (such as expansion, induration and embrittlement), the irradiation flux has to be large enough [5, 6]. Therefore, it is necessary to design a high-flux rate ion implanter to meet the demand for high dose implantation. The precise controllability over energy and dosage of implanted ions provides much feasibility and convenience for material processing and modification, and synthesis of new materials. Ion implantation processing, such as high dose and low energy ion implantation, requests innovative ion implanters of accurate energy and dose [7, 8]. Inevitably, it is essential to calibrate their implantation uniformity, for which Rutherford backscattering spectrometry (RBS) is undoubtedly a good choice.

As an important member among typical ion beam-based methods, RBS has been widely utilized in compositional and depth profiling analysis in the near-surface region [9]. It provides both quantitative and qualitative information of the elements in the surface layer, in high precision [10–12]. The quantification of RBS is related to the scattering cross-sectional  $\sigma$  and is highly dependent on the kinematic factor  $K$  of each element. Because  $\sigma$  and  $K$  values are known constants for any given projectile and scattering angle, the RBS spectroscopy can reflect the composition and thickness information of the surface

layer in a more intuitive way [13]. This makes it possible for applications on detection of surface impurities, impurity distribution in depth and thickness measurements for thin films and implanted samples [14]. For conventional RBS measurements ( $E_0 = 1\text{--}2$  MeV), depth resolution of 10–20 nm can be achieved depending on the projectiles and target materials. By optimizing energy resolution of the detector–analyzer system, the depth resolution can reach the level of sub-nanometer, which is beneficial for precise thickness analysis of thin films [15, 16]. RBS spectra are analyzed by standard ion beam analysis codes of SIMNRA [17] or DataFurnace [18]. With careful analysis and simulation, an accuracy of  $<1\%$  can be achieved for both quantification [18–20], which shows an advantage over analytical techniques using other probes, e.g., X-ray photoelectron spectroscopy and energy dispersion X-ray spectroscopy. RBS is also advantageous owing to its nondestructive measurements and easy treatment of samples.

In this paper, implantation uniformity of a newly designed ion implanter is studied by RBS, supplemented with sheet resistance measurement. Good dopant uniformity is achieved by tuning the mode of electrostatic scanning.

## 2 Experimental

The Ar ions were implemented into boron-doped Si (001) wafers ( $\Phi 10$  cm) at 190 keV to a dose of  $3 \times 10^{16}$  atoms/cm<sup>2</sup> on an ion implanter manufactured by the Zhongkexin Electronics Equipment Co. Ltd. Its design, without the use of  $7^\circ$  electrostatic deflection, adopts an electrostatic scanning strategy which ensures uniformity of the ion implantation while taking advantage of neutral particles to reach a high implantation dose.

Then, the implanted Si wafers were cut into several 1 cm  $\times$  1 cm samples labeled with their positions. They were measured at an RBS angle of  $170^\circ$  using  $\text{Li}^{2+}$  ion beams of 2.75 or 2.45 MeV in normal incidence. The RBS data were analyzed by using the SIMNRA code, which directly gave the implantation dose and thickness of the implanted layer. The accurate pileup model and double scattering model were applied in the simulation, along with Andersen cross sections and Ziegler/Biersack stopping power database.

Sheet resistance measurements were subsequently applied at room temperature on the Ar-implanted Si samples, so as to validate the RBS results. The sheet resistance measurements were conducted with the van der Pauw configuration using ohmic contact indium electrodes, with a voltage range of  $-1$  to 1 V.

## 3 Results and discussion

The RBS measurements for the ion-implanted Si wafer  $A_1$  was performed by using 2.75 MeV  $\text{Li}^{2+}$  ions as the projectiles with a net ion beam accumulation of  $\sim 3$   $\mu\text{C}$ . Energy of the incident beams was calibrated by using the nuclear reaction of  $\text{C}(\text{p}, \text{p})\text{C}$  at 1.74 MeV, with an uncertainty of  $<0.5\%$ . The uncertainty caused by the counting statistics is about 3%, and the live time correction was accomplished during simulation with the dead time of 4%.

Figure 1a shows the RBS spectra obtained at different spots on the wafer, which are schematically shown in the insert. It can be seen that the classical RBS spectra clearly reveal the information for elements Ar and Si. The positions of Ar and Si are perfectly corresponding to their kinetic factor  $K$  at this scattering angle for this specific projectile. Usually for ion-implanted samples, the dose of implanted ions with a perpendicularly incident beam can be expressed as [14]:

$$(N_t)_{\text{imp}} = A_{\text{imp}} \sigma_{\text{sub}}(E_0) \cdot \xi / \{ H_{\text{sub}} \sigma_{\text{imp}}(E_0) \cdot [\varepsilon_0]_{\text{sub}} \}, \quad (1)$$

where  $A_{\text{imp}}$  is the total number of detected ions implanted;  $H_{\text{sub}}$  is the substrate surface height of signal;  $\sigma_{\text{imp}}$  and  $\sigma_{\text{sub}}$  are the scattering cross sections of the implanted ions and substrate, respectively;  $\xi$  is the energy width of a channel; and  $[\varepsilon_0]_{\text{sub}}$  is the stopping cross-sectional factor of the substrate. In this case, the  $\sigma_{\text{sub}}$ ,  $\sigma_{\text{imp}}$ ,  $\xi$  and  $[\varepsilon_0]_{\text{sub}}$  are constant values, while  $A_{\text{imp}}$  can be approximated as the surface height of Ar signal  $H_{\text{Ar}}$ , because of the identical experimental conditions. Therefore, we have,

$$(N_t)_{\text{Ar}} \propto H_{\text{Ar}}/H_{\text{Si}} \quad (2)$$

In Fig. 1a, the  $H_{\text{Si}}$  is of obvious discrepancy, showing that the implanted Ar ions are not uniformly distributed in the Si substrate.

Figure 1b shows the simulated RBS spectrum for Spot  $A_{11}$ , which is located at a distance of 1.5 cm from the wafer edge (the same as  $A_{12}$ ,  $A_{14}$  and  $A_{15}$ ). The good matching between simulated and experimental data shows the feasibility and accuracy of the evaluation of implanted doses by the present method. According to the simulation results, the implanted Ar dose at  $A_{11}$  is  $3.8 \times 10^{16}$  atoms/cm<sup>2</sup>.

In fact, the great discrepancy and poor homogeneity (up to 16%) on implantation doses between different spots arise from design drawback of the ion implanter. Due to lack of the  $7^\circ$  electrostatic deflector, most neutral ions can easily reach the sample, as they cannot be deflected by the electrostatic scanner. To solve this problem, the electric scanner of the ion implanter was tuned by a programmed variation of the retention time for different sites, i.e., the sweeping of scanning is sped down while the ion beams reach the sample edge, but sped up while it reaches the

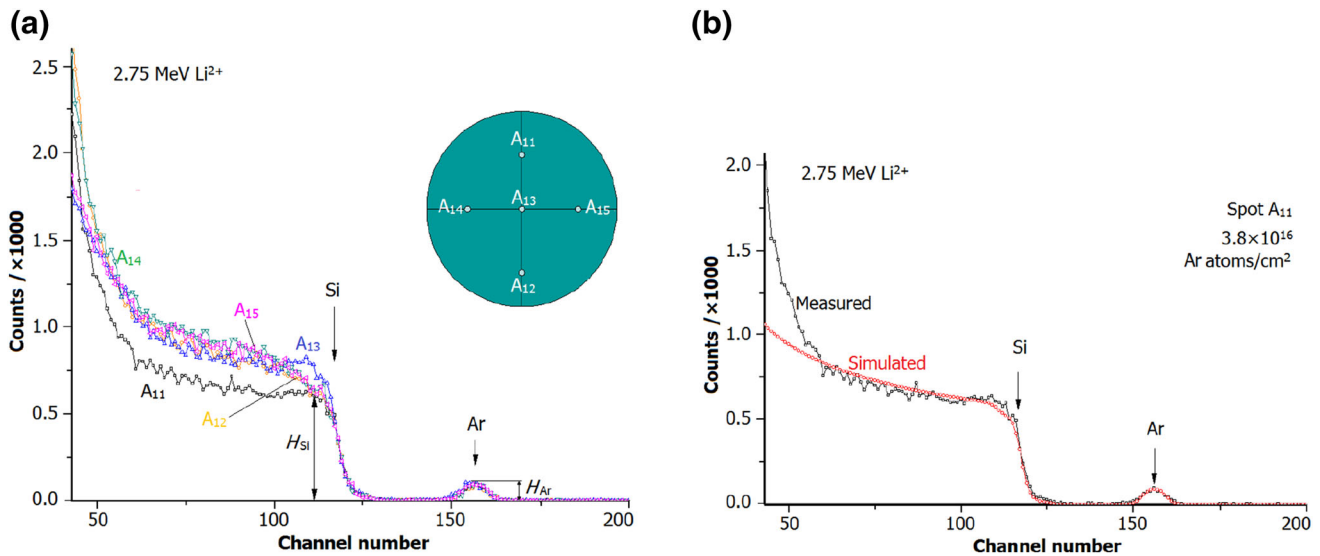


**Fig. 1** RBS spectra of sample  $A_1$  measured at different positions (a) and the measured and simulated spectra of Spot  $A_{11}$  (b)

sample center. In this way, Sample  $B_1$  was implanted at the same energy and dose as Sample  $A_1$ , but running in the new scanning mode. The RBS measurements for  $B_1$  were conducted with normal incidence 2.45 MeV  $\text{Li}^{2+}$  ion beam as the projectile with the detector mounted at  $170^\circ$ .

Figure 2a shows the measured RBS spectra of the nine spots ( $B_{11}$ – $B_{19}$ ) on Sample  $B_1$ , among which  $B_{11}$  is located at the center, while  $B_{12}$ – $B_{15}$  and  $B_{16}$ – $B_{19}$  are evenly located at the concentric circles with diameter of 1.5 and 3.0 cm, respectively. From the similar ratios of  $H_{\text{Ar}}/H_{\text{Si}}$ , the implanted Ar ions distributed much more uniformly (to an homogeneity of 3.25 %) in the Si substrate after calibrating the electric scanning mode. The simulated spectrum at spot

$B_{13}$  is shown in Fig. 2b, which gives the Ar dose of  $3.04 \times 10^{16}$  atoms/ $\text{cm}^2$ , which is in close proximity to the preset value  $3.0 \times 10^{16}$  atoms/ $\text{cm}^2$  of the ion implanter. This indicates our success in improving the ion implantation uniformity.

To verify the accuracy of SIMNRA simulation, the Samples  $A_1$  and  $B_1$  were processed by plating indium onto the four corners to fabricate ohmic contact electrodes in the van der Pauw configuration for sheet resistance measurements. The obtained sheet resistances of Samples  $A_1$  and  $B_1$  are plotted in Fig. 3a, b, respectively. It can be seen that the tendency of the sheet resistance values agrees well with that of the dose values evaluated from the RBS spectra, with the

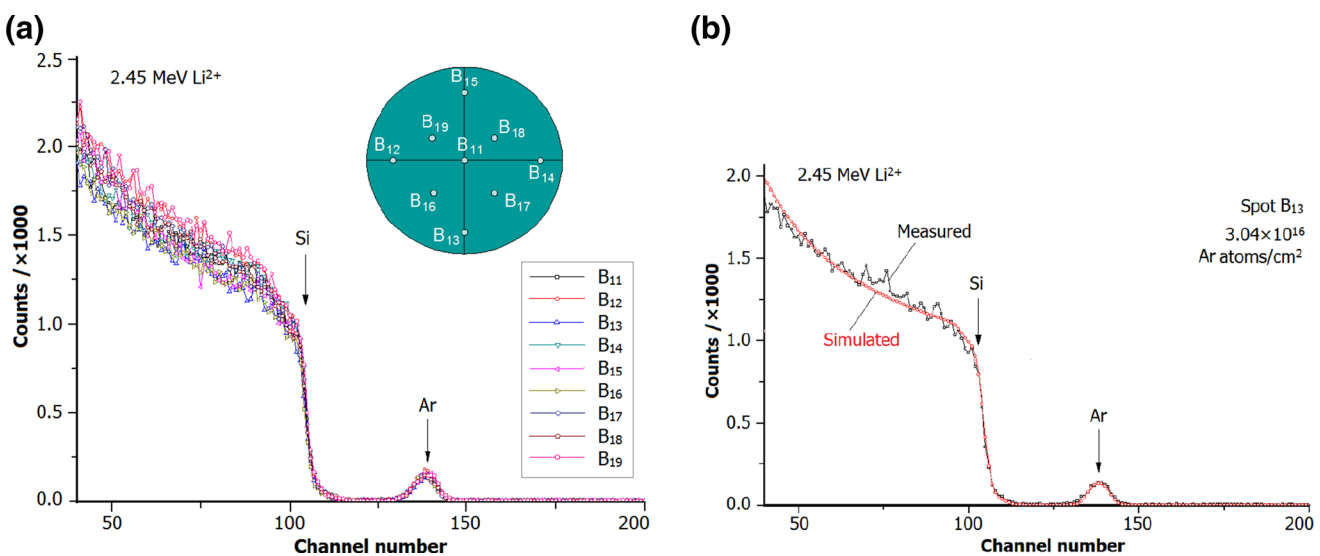


**Fig. 2** RBS spectra of Sample  $B_1$  measured at different positions (a) and the measured and simulated spectra at Spot  $B_{13}$  (b)

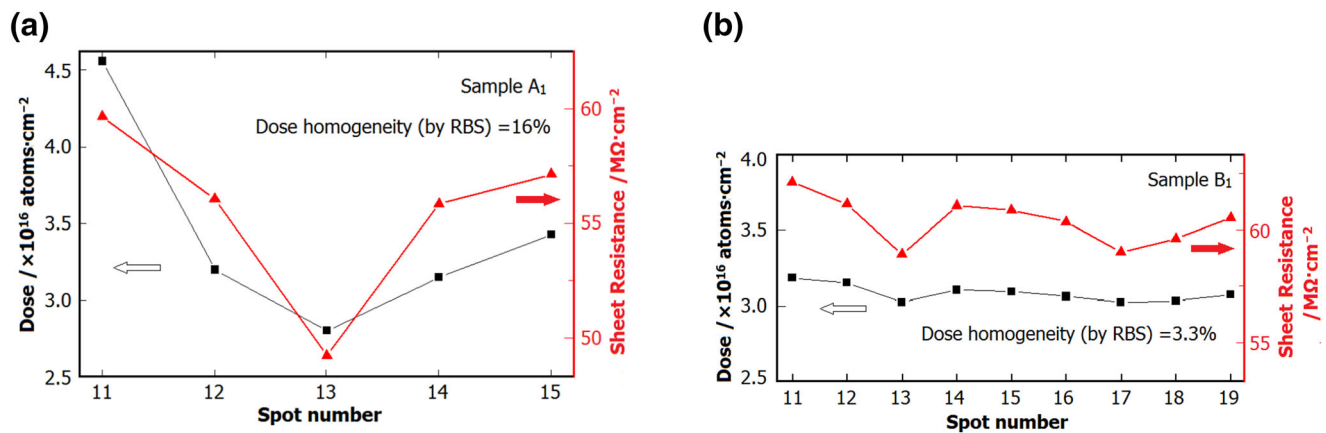


**Fig. 3** SIMNRA simulated Ar doses and sheet resistances obtained from sheet resistance measurement for A<sub>1</sub> (a) and B<sub>1</sub> (b)

former decreases less than the latter. This can be attributed to two reasons. First, the Ar ion implantation would inevitably create energy levels in the forbidden gap and remove or trap the carriers. Second, the ion implantation process would induce amorphization of the Si substrate, which significantly reduces the carrier mobility by scattering.

The well-supported sheet resistance results demonstrate the feasibility of evaluating the implantation uniformity of an ion implanter. However, a prime advantage of evaluating the implantation uniformity by RBS is that it gets rid of the cumbersome procedure of fabricating the ohmic contact electrodes. Next, RBS is never limited by the sizes and shapes of the samples. Finally, RBS overcomes the fatal flaw in sheet resistance measurements which work well just in the very surface region. Therefore, RBS is undoubtedly a more appropriate and nondestructive method for uniformity calibration of the ion implantation system.

## 4 Conclusion

In conclusion, the implantation uniformity of the newly designed LC-16 ion implanter was studied by both RBS and sheet resistance measurements. Through SIMNRA simulation of the experimental spectra, RBS directly gave the dose values with good precision with respect to the preset dosages. And the RBS results were confirmed by sheet resistance measurements. Though the latter method gave good tendency, it reflected the ion dose indirectly (via the sheet resistance). Therefore, RBS is a direct technique for measuring ion-implanted samples, with convenience and precision, and the uniformity of the ion implanter has been successfully calibrated by the RBS method. This calibration paves the way for application of the ion implanter for doping and irradiation of materials.

## References

1. K.K. Tiong, P.M. Amirtharaj, F.H. Pollak et al., Effects of As<sup>+</sup> ion implantation on the Raman spectra of GaAs: "Spatial correlation" interpretation. *Appl. Phys. Lett.* **44**, 122 (1984). doi:10.1063/1.94541
2. J.R. Conrad, J.L. Radtke, R.A. Dodd et al., Plasma source ion-implantation technique for surface modification of material. *J. Appl. Phys.* **62**, 4591 (1987). doi:10.1063/1.339055
3. O. Diwald, T.L. Thompson, E.G. Goralski et al., The effect of nitrogen ion implantation on the photoactivity of TiO<sub>2</sub> rutile single crystals. *J. Phys. Chem. B* **108**, 52–57 (2004). doi:10.1021/jp030529t
4. A. Meldrum, R.F. Haglund JR et al., Nanocomposite materials formed by ion implantation. *Adv. Mater.* **13**, 1431–1444 (2001). doi:10.1002/1521-4095(200110)13:19<1431:AID-ADMA1431>3.0.CO;2-Z
5. M.Q. Hong, F. Ren, H.X. Zhang et al., Enhanced radiation tolerance in nitride multilayered nanofilms with small period-thicknesses. *Appl. Phys. Lett.* **101**, 153117 (2012)
6. M.Q. Hong, Y.Q. Wang, F. Ren et al., Helium release and amorphization resistance in ion irradiated nanochannel films. *EPL* **106**, 12001 (2014). doi:10.1209/0295-5075/106/12001
7. H. Tsuji, S. Kido, H. Sasaki et al., Negative-ion implanter for powders and its application to nanometer-sized metal particle formation in the surface of glass beads. *Rev. Sci. Instrum.* **71**, 804 (2000). doi:10.1063/1.1150299
8. T.K. Chini, D. Datta, S.R. Bhattacharyya et al., Nanostructuring with a high current isotope separator and ion implanter. *Appl. Surf. Sci.* **182**, 313–320 (2001). doi:10.1016/S0169-4332(01)00420-2
9. L.C. Feldman, J.W. Mayer, *Fundamentals of Surface and Thin Film Analysis. Chap. 5* (North-Holland, Amsterdam, 1986)
10. N.S. Saleh, K.A. Al-Saleh, D.E. Arafah et al., Combined nuclear measurements of yeast. *Nucl. Instrum. Methods B* **23**, 379 (1987). doi:10.1016/0168-583X(87)90395-8
11. E. Rauhala, J. Raisanen, M. Luomajarvi, An external beam method for ion backscattering. *Nucl. Instrum. Methods B* **6**, 543 (1985). doi:10.1016/0168-583X(85)90015-1
12. T. Cichocki, D. Heck, L. Jarczyk et al., Proton microbeam study of calcium-phosphate complexes in human arteries. *Nucl. Instrum. Methods B* **22**, 210 (1987). doi:10.1016/0168-583X(87)90329-6

13. J. Demeulemeester, D. Smeets, C. Van Bockstael et al., Pt redistribution during Ni(Pt) silicide formation. *Appl. Phys. Lett.* **93**, 261912 (2008). doi:[10.1063/1.3058719](https://doi.org/10.1063/1.3058719)
14. W.K. Chu, J.W. Mayer, M.A. Nicolet, *Backscattering Spectrometry* (Academic press, New York (USA), 1978)
15. W. Roessler, D. Primetzhofner, P. Bauer, Analysis of Mo/Si multilayers by means of RBS. *Nucl. Instrum. Methods B* **317**, 126–129 (2013). doi:[10.1016/j.nimb.2012.12.084](https://doi.org/10.1016/j.nimb.2012.12.084)
16. H. Hashimoto, A. Ohno, K. Nakajima et al., Surface characterization of imidazolium ionic liquids by high-resolution Rutherford backscattering spectroscopy and X-ray photoelectron spectroscopy. *Surf. Sci.* **604**, 464–469 (2010). doi:[10.1016/j.susc.2009.12.023](https://doi.org/10.1016/j.susc.2009.12.023)
17. M. Mayer, SIMNRA, a simulation program for the analysis of NRA, RBS and ERDA. *AIP Conf. Proc.* **475**, 541 (1999). doi:[10.1063/1.59188](https://doi.org/10.1063/1.59188)
18. N.P. Barradas, C. Jeynes, R.P. Webb, Simulated annealing analysis of Rutherford backscattering data. *Appl. Phys. Lett.* **71**, 291 (1997). doi:[10.1063/1.119524](https://doi.org/10.1063/1.119524)
19. J.L. Colaux, C. Jeynes, K.C. Heasman et al., Certified ion implantation fluence by high accuracy RBS. *Analyst* **140**, 3251 (2015). doi:[10.1039/c4an02316a](https://doi.org/10.1039/c4an02316a)
20. C. Jeynes, N.P. Barradas, E. Szilágyi, Accurate determination of quantity of material in thin films by Rutherford backscattering spectrometry. *Anal. Chem.* **84**(14), 6061–6069 (2012). doi:[10.1021/ac300904c](https://doi.org/10.1021/ac300904c)